

RESEARCH ARTICLE

Does elevated glucose metabolism correlate with higher cell density in Neurofibromatosis type 1 associated peripheral nerve sheath tumors?

Dominik Berzaczy^{1*}, Marius E. Mayerhoefer¹, Amedeo A. Azizi², Alexander R. Haug³, Daniela Senn³, Dietrich Beitzke¹, Michael Weber¹, Tatjana Traub-Weidinger³

1 Department of Biomedical Imaging and Image-guided Therapy, Division of General and Pediatric Radiology, Medical University of Vienna, Waehringer Guertel, Vienna, Austria, E.U, **2** Department of Pediatrics and Adolescent Medicine, Medical University of Vienna, Waehringer Guertel, Vienna, Austria, E.U, **3** Department of Biomedical Imaging and Image-guided Therapy, Division of Nuclear Medicine, Medical University of Vienna, Waehringer Guertel, Vienna, Austria, E.U

* dominik.berzaczy@meduniwien.ac.at



OPEN ACCESS

Citation: Berzaczy D, Mayerhoefer ME, Azizi AA, Haug AR, Senn D, Beitzke D, et al. (2017) Does elevated glucose metabolism correlate with higher cell density in Neurofibromatosis type 1 associated peripheral nerve sheath tumors? PLoS ONE 12 (12): e0189093. <https://doi.org/10.1371/journal.pone.0189093>

Editor: Gayle E. Woloschak, Northwestern University Feinberg School of Medicine, UNITED STATES

Received: June 26, 2017

Accepted: November 17, 2017

Published: December 5, 2017

Copyright: © 2017 Berzaczy et al. This is an open access article distributed under the terms of the [Creative Commons Attribution License](https://creativecommons.org/licenses/by/4.0/), which permits unrestricted use, distribution, and reproduction in any medium, provided the original author and source are credited.

Data Availability Statement: All relevant data are within the paper and its Supporting Information files.

Funding: This work was supported by the Austrian Science Fund (FWF), project number KLIF 382 to Marius E. Mayerhoefer. <https://www.fwf.ac.at/en/>.

Competing interests: The authors have declared that no competing interests exist.

Abstract

Purpose

To investigate whether elevated glucose metabolism in neurofibroma, determined by [F18]-FDG-PET, is correlated with cell density in MRI, as expressed through the apparent diffusion coefficient.

Materials and methods

Patients diagnosed with neurofibromatosis type 1 and peripheral nerve sheath tumors (PNST) were enrolled in this prospective, IRB-approved study. After a single [F18]-FDG injection, patients consecutively underwent [F18]-FDG-PET/CT and [F18]-FDG-PET/MRI on the same day. Maximum and mean standardized uptake values (SUV_{max}, SUV_{mean}) on [F18]-FDG-PET/CT and [F18]-FDG-PET/MRI were compared, and correlated with minimum and mean apparent diffusion coefficients (ADC_{mean}, ADC_{min}).

Results

A total of 12 (6 male/6 female, mean age was 16.2 ± 5.2 years) patients were prospectively included and analyzed on a per-lesion (n = 39) basis. The SUV_{mean} of examined PNST showed a moderate negative correlation with the ADC_{mean} (r = -.441) and ADC_{min} (r = -.477), which proved to be statistically significant (p = .005 and p = .002). The SUV_{max} of the respective lesions, however, showed a weaker negative correlation for ADC_{mean} (r: -.311) and ADC_{min} (r: -.300) and did not reach statistical significance (p = .054 and p = .057).

Lesion-based correlation between [F18]-FDG-PET/MRI and [F18]-FDG-PET/CT showed a moderate correlation for SUV_{max} (r = .353; p = .027) and a strong one for SUV_{mean} (r = .879; p = .001). Patient-based liver uptake (SUV_{max} and mean) of [F18]-FDG-PET/MRI and [F18]-FDG-PET/CT were strongly positively correlated (r = .827; p < .001 and r = .721; p < .001) but differed significantly (p < .001).

Conclusions

We found a statistically significant, negative correlation between glucose metabolism and cell density in PNST. Thus, ADC_{mean} and ADC_{min} could possibly add complimentary information to the SUV_{max} and SUV_{mean} and may serve as a potential determinant of malignant transformation of PNST.

Introduction

Neurofibromatosis type 1 (NF1) is an autosomal dominant neurocutaneous disorder caused by a mutation of the tumor suppressor gene NF1 (17q11.2) with a rate of approximately 1 in 3000 live births [1–3]. NF1 is a tumor pre-disposition syndrome, i.e. patients carry a high risk of developing benign and malignant tumors [4–6]. Diagnosis is made genetically or clinically using the NIH criteria which are based on typical features such as Café au lait macules, neurofibroma, optic pathway glioma, iris hamartoma (Lisch nodules) and osseous dysplasia [7].

Neurofibroma most commonly show cutaneous or subcutaneous, focal dermal growth or can be located adjacent to the spine or intraforaminal and may appear as nodular or diffuse plexiform neurofibroma. The latter are of particular importance as they have an increased risk of malignant transformation with a lifetime risk that has been reported from 5 to 13% [8,9].

These malignant peripheral nerve sheath tumors (MPNST) are difficult to detect as malignant transformed tissue is often embedded within benign lesions [10].

When present, MPNST show a poor prognosis with an overall 5-year-survival of about 42% due to delayed diagnosis, early metastasis (liver, lung, brain, lymph nodes and bones) and limited response to systematic therapy [3,5,8,9,11].

Patients with NF1 therefore demand increased surveillance. Surgical resection is technically challenging due to the anatomic location of these tumors, not only as the mainstay of therapy, but also when obtaining a histological specimen for diagnostic purposes. Morphologic imaging parameters of these tumors obtained by contrast-enhanced computed tomography (CE-CT) and magnetic resonance imaging (MRI) cannot determine malignant transformation to a satisfactory extent. Repeated biopsies, on the other hand, are uncommon in the clinic and obviously, no acceptable option. Nowadays, [F18]fluoro-2-deoxy-D-glucose-positron emission tomography ([F18]-FDGPET) imaging is in use to help differentiate between benign and malignant PNST in patients with NF 1. To the best of our knowledge, no data have been published concerning a correlation between the standardized uptake value (SUV) and apparent diffusion coefficient (ADC) in peripheral nerve sheath tumors in the setting of NF 1 obtained simultaneously using [F18]-FDG-PET/MRI.

Purpose of this report was to investigate whether glucose metabolism in plexiform neurofibroma, determined by [F18]-FDG-PET, is correlated with cell density on diffusion-weighted MRI (DWI), as expressed through the ADC, which may represent a complimentary imaging-derived biomarker to detect MPNST.

Materials and methods

Patient population and study design

Pediatric, adolescent and young adult patients diagnosed with neurofibromatosis type 1 and peripheral nerve sheath tumors, were enrolled in this prospective, Institutional Review Board (ethics committee of the medical university of vienna) approved, dual-modality study. Written informed consent was obtained from all adult patients and, in case of minor participants, from

their guardians, prior to imaging. After a single [F18]-FDG injection, patients consecutively underwent [F18]-FDG-PET/CT and [F18]-FDG-PET/MRI on the same day, for initial staging or follow-up purposes. General contraindications to MRI (e.g., severe claustrophobia, unsafe metal implants for a field strength of 3T), elevated glucose levels (>150mg/dl), pregnancy and known adverse reactions to ionized contrast media served as exclusion criteria.

Imaging protocols

[F18]-FDG-PET/CT and [F18]-FDG-PET/MRI were performed consecutively on the same day, using only a single injection of [F18]-FDG for both examinations.

[F18]-FDG-PET/CT was generally performed first, covering the anatomy from head to toe, using a 64-row multi-detector hybrid PET/CT device (Biograph TruePoint 64; Siemens, Erlangen, Germany). For PET, this scanner offers an axial field-of-view of 216 mm, a sensitivity of 7.6 cps/kBq, and a transaxial resolution of 4–5 mm. After patients had fasted for five hours, PET was performed 45–60 min after an intravenous administration of a mean of 225 ± 64 MBq of [F18]-FDG, with a 3-min/bed position, four iterations, and 21 subsets, a 5-mm slice thickness, and a 168x168 matrix, using the point-spread function (PSF)-based reconstruction algorithm TrueX. Venous-phase CE-CT was used for attenuation correction, and was obtained after the intravenous injection of a mean of 74 ml of a tri-iodinated, non-ionic contrast medium (adjusted to body weight) at a rate of 2 ml/s; a tube current of 120 mA; a tube voltage of 230kV; a collimation of 24x1.2 mm; a 3-mm slice thickness with a 2-mm increment; and a 512x512 matrix. In 4 cases a low dose CT protocol was applied using 120Kv and 50mAs without any contrast media.

[F18]-FDG-PET/MRI, covering the anatomy from the vertex to the upper thigh was performed directly after PET/CT, using an integrated, simultaneous, hybrid PET/MRI device (Biograph mMR; Siemens, Erlangen, Germany) operating at 3 Tesla, with high-performance gradient systems (45 mT/m) and a slew rate of 200 T/m/s, and equipped with a phased-array body coil.

For PET, the system offers an axial FOV of 256 mm, a sensitivity of 13.2 cps/kBq, and a transaxial resolution of 4.4 mm. PET was performed 100–150 min after the original tracer administration, with a 5-min/bed position, three iterations, and 21 subsets, a 4.2-mm slice thickness, and a 172x172 matrix, using the point spread function-based reconstruction algorithm HD-PET.

A coronal T1-weighted (T1w) two-point DIXON breath-hold MR sequence (VIBE) was acquired for attenuation correction, using the following parameters: repetition time (TR)/echo times (TE) 3.6/TE1 = 1.23 ms TE2 = 2.46 ms; one average, two echoes; a 10° flip angle; a 320x175 matrix with a 430x309 mm FOV; and a 3-mm slice thickness with 0.6-mm gap.

For anatomic correlation an axial VIBE, with the following parameters was used: repetition time (TR)/echo times (TE), 4.9/2.1ms; one average, a 9° flip angle; a 172x320 matrix with a 273x380 mm FOV; and a 3-mm slice thickness with 0.6-mm gap.

A single-shot, echo-planar imaging (EPI)-based, spectral adiabatic inversion recovery (SPAIR) diffusion-weighted imaging (DWI) sequence was obtained with the following parameters: b-values, 50 and 800; TR/TE, 6600/63 ms; six averages and one echo; a 180° flip angle; a 168x104 matrix with a 440x340 mm FOV; and a 6-mm slice thickness with a 1.2-mm gap.

Qualitative and quantitative image analysis

A board-certified radiologist and a board-certified nuclear medicine physician performed all image analyses in consensus (side-by-side reading) to guarantee that the same lesions were chosen for the quantitative analysis on PET and DWI.

In a first step, to correlate FDG PET and DWI of PETMRI, a maximum of 5 PNST lesions per patient, localized adjacent to nerve fascicles that arise from major nerve branches, that had to be visible on T1w and DWI with a 2cm minimum long axis diameter were defined. Their corresponding maximum and mean standardized uptake values (SUV_{max} and mean) were measured on [F18]-FDG-PET based on isocontour volumes of interest (VOIs) that included all voxels above 50% of the SUV_{max} of each lesion, and were constructed using the Syngo MultiModality Workplace environment (Siemens, Erlangen, Germany). Similarly, minimum and mean apparent diffusion coefficients (ADC_{min} and ADC_{mean}, ($\times 10^{-6}$ mm²/s)) of respective lesions were measured on ADC maps, using the interactive level-set method of the MIPAV 7.2.0 software package (Center for Information Technology, NIH, USA).

Secondly, solely for comparison of the PET components of PETCT and PETMR, the SUV values of the largest lesion visible both on CT and T1w images in PETMR, as well as the SUVs of the liver parenchyma were measured by placing spherical volumes of interest (VOIs) with a 2-cm diameter over the lesion and over a lesion-free part of the liver parenchyma, respectively.

Statistical analysis

Pearson correlation coefficients (r) were used to assess the relationship between liver parenchymal and lesional uptake in [F18]-FDG-PET/MRI and [F18]-FDG-PET/CT, and between the imaging-derived parameters SUV_{max} and SUV_{mean} and the respective ADC values, on a per-lesion basis, on [F18]-FDG-PET/MRI. Continuous variables are expressed as arithmetic mean \pm standard deviation (SD). Categorical variables are presented as absolute frequencies. Paired t-tests were performed to compare SUV_{max} and SUV_{mean} values measured on PET/MRI and PET/CT, respectively. The level of significance was set to $p \leq .05$ for all tests. Statistical tests were performed using IBM SPSS Statistics 21.0 software (IBM Corp., Armonk, NY, USA).

Results

Patients

A total of twelve patients—six males and six females—with a total of 39 lesions were prospectively included between January 2014 and June 2015. The mean age was 16.2 ± 5.2 (SD) years.

Correlation of SUV and ADC

These calculations were performed on a per-lesion basis (up to five different PNST loci per patient).

The SUV_{mean} showed a statistical significant moderate negative correlation with the ADC_{mean} ($r = -.441$, $p = .005$) and ADC_{min} ($r = -.477$, $p = .002$).

However, the SUV_{max} of the respective lesions showed a weaker negative correlation for ADC_{mean} ($r = -.311$, $p = .054$) and ADC_{min} ($r = -.300$, $p = .057$), and only showed a trend towards statistical significance (Fig 1).

Correlation of the PET components of [F18]-FDG-PET/MRI and [F18]-FDG-PET/CT

SUV_{mean} showed a strong, statistical significant correlation ($r = .879$; $p = .001$) as SUV_{max} showed a moderate, also statistical significant correlation ($r = .353$; $p = .027$) between the PET components of both techniques.

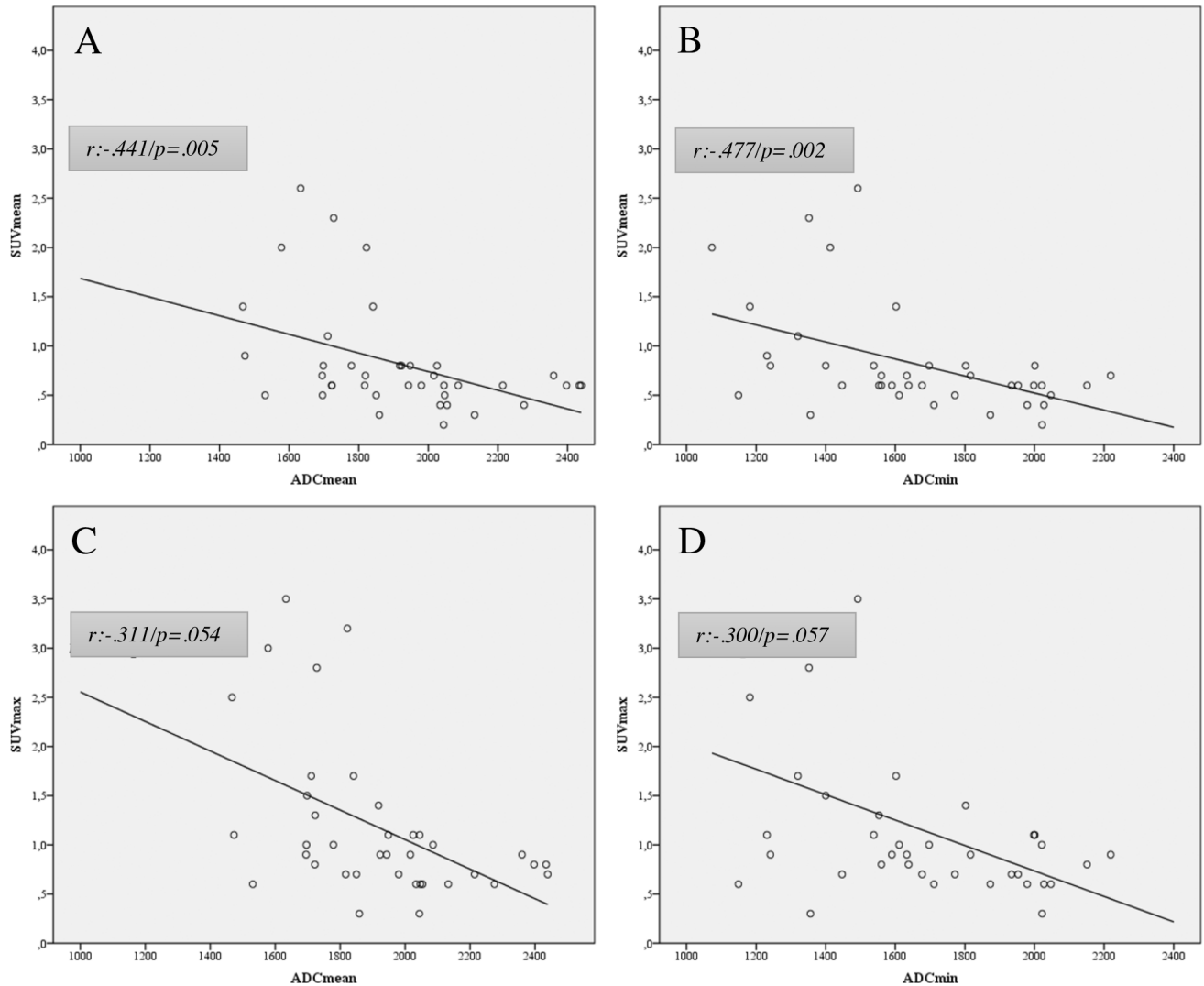


Fig 1. Correlation of glucose metabolism and cell density in PET/MRI. (A and B) SUVmean showed a moderate, inverse correlation to ADC mean and min. (C and D) SUVmax showed a weak inverse correlation for and ADC mean and min.

<https://doi.org/10.1371/journal.pone.0189093.g001>

Patient-based liver uptake (SUVmax and SUVmean) of [F18]-FDG-PET/MRI and [F18]-FDG-PET/CT was found to be strongly positively correlated ($r = .827$; $p < .001$; and $r = .721$; $p < .001$) but differed significantly for both SUVmax and SUVmean ($p < .001$) (Fig 2).

Discussion

Determination of malignant transformation in peripheral nerve sheath tumors is a challenging task on many levels. The use of either clinical symptoms, that suggest malignancy (e.g. neurological deficits, fast increasing tumor volume, new onset pain lasting for more than four weeks) or imaging modalities only assessing morphologic parameters provide only very limited ability to characterize these tumors and may not be specific enough to differentiate between benign and malignant peripheral nerve sheath tumors (PNSTs). MPNST are highly aggressive tumors that represent a frequent cause of death in these patients [12]. Hence, these tumors warrant early diagnosis to allow early, potential curative therapy. Therefore, non-invasive diagnostic imaging methods are highly desirable.

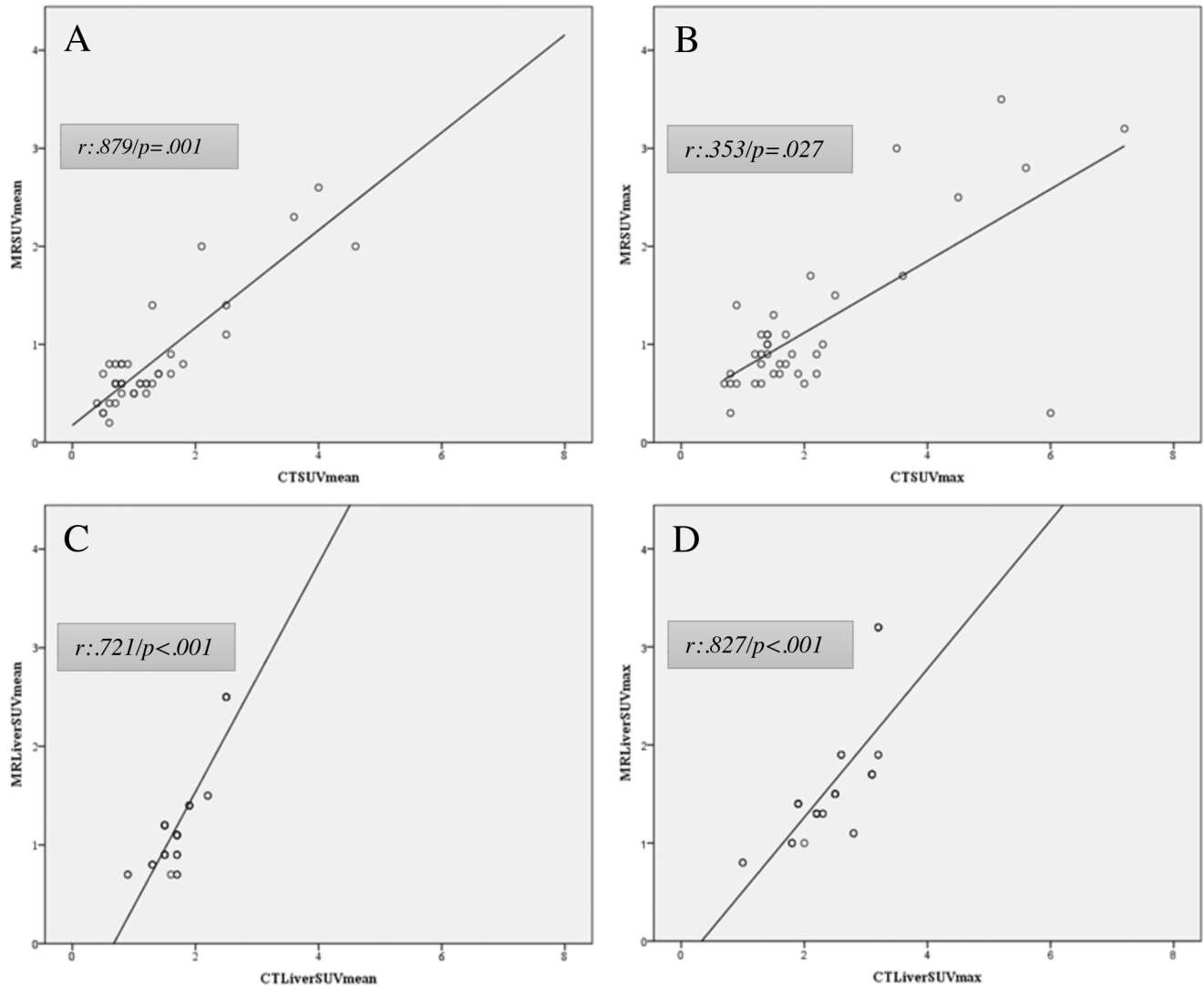


Fig 2. Correlation of the PET component of PET/MRI and PET/CT. (A) SUVmean showed a strong positive correlation and (B) SUVmax a moderate positive correlation for PET/MRI and PET/CT. (C and D) SUV mean and max showed a strong positive correlation for patient-based liver uptake.

<https://doi.org/10.1371/journal.pone.0189093.g002>

Today, [F18]-FDG-PET/CT is a well-established imaging modality, which is most commonly used in clinical routine in staging, restaging, therapy monitoring and to help identifying possible MPNSTs in symptomatic NF1 patients, offering a high sensitivity [13].

[F18]-FDG-PET imaging allows a semi-quantitative measure of glucose metabolism and calculation of SUV and its derived parameters that reflect increased metabolic activity and levels of overexpression of its respective receptors. However, the crucial point of identification of malignant transformation by using a distinctive SUVmax as cutoff to differentiate between benign and malignant plexiform neurofibroma remains not fully clear and recent literature reports varying results regarding [F18]-FDG imaging [3,6].

Literature reports optimal cut-off values, with regard to maximized sensitivity and specificity, ranging from 3.1 to 6.1 [13–17].

Tovmassian et al. [3] report in a recent review, that most of proposed cut-off values for SUVmax are found between 3 and 4, which is a range in that both benign and malignant

PNSTs can occur and hence makes clinical decision making difficult. Furthermore, the SUVmax can be influenced by multiple factors arising from the use of different scanners, variability in technical parameters, and image reconstruction and calibration [18]. However, a SUVmax > 3.5 is commonly used in clinical practice and research in this regard.

Azizi et al. [19] recently published a study comprising data on symptomatic and asymptomatic NF1 patients showing the value of FDG PET in the work-up of NF1 patients.

Promising approaches to investigate alternative or complimentary imaging derived markers to SUVmax have been published recently. Salamon et al. [20] reported an increased specificity using a SUVmax tumor-to-liver (TTL) ratio of 90.3% in attempt to overcome the variability of the SUVmax. The same group published data showing a statistically significant higher rate of metabolic tumor volume (MTV) and total lesion glycolysis (TLG) in MPNSTs. In support of this data Van der Gucht et al. [21] could show the utility of TLG as prognostic marker for survival when compared to TTL and the SUVmax. Chirindel et al. [22] also showed good clinical utility of [F18]-FDG-PET when using lesion to liver activity normalization when comparing early and delayed imaging which yielded similar accuracy in qualitative interpretation of neurofibroma. However, SUVmax, despite its limitations, seems to be the most useful parameter in [F18]-FDG-PET based on available data in literature [3].

With the advent of hybrid PET/MRI scanners, a hybrid imaging method that combines metabolic PET information and DWI in a single examination became available for clinical practice. In this preliminary study we investigated whether (semi)-quantitative measures of SUVs and ADCs derived from [F18]-FDG-PET and DWI are correlated. As sarcomatous tissue shows an increased glucose metabolism that is believed to be linked to a higher cell density and lower differentiation grade, a correlation of both parameters seems a valid approach. Furthermore, we investigated how the PET components of [F18]-FDG-PET/CT and [F18]-FDG-PET/MRI correlate to provide connecting data on both imaging methods in these consecutively performed examinations.

As our main result we found a moderate, statistically significant negative correlation of the SUVmean of examined peripheral nerve sheath tumors with the ADCmean and ADCmin (Figs 3 and 4).

These results are comparable to published findings of inverse correlation between SUVs and ADCs that have been reported in varying degrees and in different tumor entities. Schaarschmidt et al. found a significant inverse correlation in metastatic lymph nodes in NSCLC between SUVmean and ADCmean as well as between SUVmax and ADCmean [23].

Other authors reported similar results with strong inverse correlations between SUVmax and ADCmin in primary cervical cancer [24], and a work by Rakheja et al. [25], comprising different malignant tumors. ADC values that, similar to the SUVmax, carry some variability depending on manufacturer and field strength, seem to offer an additional value in monitoring therapy response as they have shown superiority over SUVmax in studies including NSCLC and MALT lymphoma [26,27].

Interestingly, our results show that the SUVmax of NF1 associated nerve sheath tumors showed a rather weak, negative correlation with ADCmean and ADCmin that only showed a clear trend towards statistical significance; however, it has to be acknowledged that our sample size was possibly too small to draw definitive conclusions. Our results are in good accordance with the published literature, especially for the SUVmean, which seems advantageous to us due to its robust nature.

Comparing the PET component of [F18]-FDG-PET/MRI to [F18]-FDG -PET/CT we found a positive correlation for SUVmax and mean for the per-patient lesion and liver uptake which differed statistical significantly between the two methods. These differences are most of

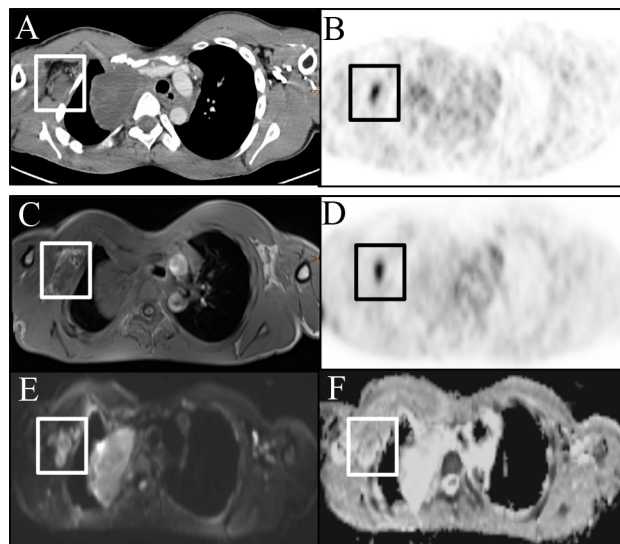


Fig 3. PNST in a 17-year male patient. (A) Peripheral nerve sheath tumor depicted on CE-CT image with (B) increased glucose metabolism. (C) Corresponding T1w image. (D) [18F]-FDG-PET depicting increased glucose uptake and corresponding restricted diffusion on (E) DWI (b800) image with (F) lowered signal on the ADC map.

<https://doi.org/10.1371/journal.pone.0189093.g003>

all due to technical differences in scatter and attenuation correction as well as different distribution of respective tracer.

Our preliminary study has limitations, the most obvious of which is the small sample size that prevented us from performing a subgroup evaluation with regard to pathohistology on a per-lesion basis. Although we found significant correlations, this fact did not allow a direct comparison between the performances of [F18]-FDG-PET and DWI.

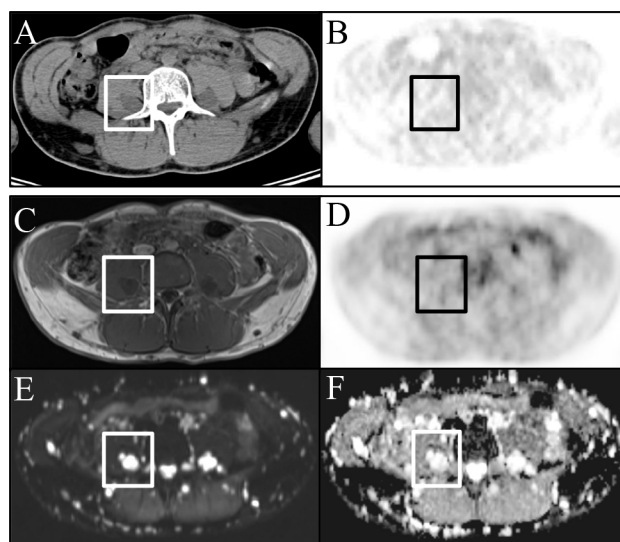


Fig 4. PNST in a 22-year male patient. (A) CE-CT image and corresponding (B) PET image with no pathological glucose uptake. (C) T1w image and corresponding (D) PET images with also no abnormal focal tracer uptake. (E) DWI (b800) and (F) ADC maps showing restricted diffusion but high signal on the ADC map.

<https://doi.org/10.1371/journal.pone.0189093.g004>

In conclusion, we found a statistically significant negative correlation between the SUV-mean and the ADCmean as well as between the SUVmean and the ADCmin in peripheral nerve sheath tumors in NF1 patients. Based on our findings we believe that a combination of the two techniques, preferably combined in the form of [F18]-FDG-PET/MRI, would possibly offer complimentary information to help characterizing PNSTs. The simultaneous acquisition of SUVs and ADCs is a good compromise between examination time and patient comfort and offers advantages in terms of clinical workflow optimization. Nevertheless, it seems obvious that discrimination between malignant and benign PNSTs and consecutive clinical decision making in NF1 patients should be based on a holistic patient-based approach, taking all available, noninvasive methods and its parameters into account. Our findings suggest that [18F]-FDG-PET and DWI offer complimentary information which might increase diagnostic accuracy, but larger cohorts to support current preliminary data are needed.

Supporting information

S1 File. Original data of the present study.
(XLSX)

Author Contributions

Conceptualization: Dominik Berzaczy, Marius E. Mayerhoefer, Dietrich Beitzke.

Data curation: Alexander R. Haug, Michael Weber.

Formal analysis: Amedeo A. Azizi, Alexander R. Haug, Michael Weber.

Funding acquisition: Marius E. Mayerhoefer.

Investigation: Amedeo A. Azizi, Dietrich Beitzke.

Methodology: Dominik Berzaczy, Dietrich Beitzke.

Project administration: Daniela Senn.

Resources: Daniela Senn.

Supervision: Tatjana Traub-Weidinger.

Validation: Michael Weber.

Visualization: Daniela Senn.

Writing – original draft: Dominik Berzaczy, Amedeo A. Azizi.

Writing – review & editing: Dominik Berzaczy, Marius E. Mayerhoefer, Alexander R. Haug, Dietrich Beitzke, Tatjana Traub-Weidinger.

References

1. Yap YS, McPherson JR, Ong CK, Rozen SG, Teh BT, Lee AS et al. The NF1 gene revisited—from bench to bedside. *Oncotarget*. 2014; 5: 5873–5892. <https://doi.org/10.18632/oncotarget.2194> PMID: 25026295
2. Uusitalo E, Rantanen M, Kallionpää RA, Pöyhönen M, Leppävirta J, Ylä-Outinen H, et al. Distinctive Cancer Associations in Patients With Neurofibromatosis Type 1. *J Clin Oncol*. 2016; 34: 1978–1986. <https://doi.org/10.1200/JCO.2015.65.3576> PMID: 26926675
3. Tovmassian D, Abdul Razak M, London K. The Role of [18F]FDG-PET/CT in Predicting Malignant Transformation of Plexiform Neurofibromas in Neurofibromatosis-1. *Int J Surg Oncol*. 2016; 2016: 6162182. <https://doi.org/10.1155/2016/6162182> PMID: 28058117

4. Pemov A, Li H, Patidar R, Hansen NF, Sindiri S, Hartley SW, Wei JS, et al. The primacy of NF1 loss as the driver of tumorigenesis in neurofibromatosis type 1-associated plexiform neurofibromas. *Oncogene*. 2017; 36: 3168–3177. <https://doi.org/10.1038/onc.2016.464> PMID: 28068329
5. Salamon J, Papp L, Tóth Z, Laqmani A, Apostolova I, Adam G, et al. Nerve Sheath Tumors in Neurofibromatosis Type 1: Assessment of Whole-Body Metabolic Tumor Burden Using F-18-FDG PET/CT. *PLoS One*. 2015; 10: e0143305. <https://doi.org/10.1371/journal.pone.0143305> PMID: 26625155
6. Ferner RE, Gutmann DH. International consensus statement on malignant peripheral nerve sheath tumors in neurofibromatosis. *Cancer Res*. 2002; 62: 1573–1577. PMID: 11894862
7. Ferner RE, Huson SM, Thomas N, Moss C, Willshaw H, Evans DG, et al. Guidelines for the diagnosis and management of individuals with neurofibromatosis 1. *J Med Genet*. 2007; 44: 81–88. <https://doi.org/10.1136/jmg.2006.045906> PMID: 17105749
8. Ducatman BS, Scheithauer BW, Piepgras DG, Reiman HM, Ilstrup DM. Malignant peripheral nerve sheath tumors. A clinicopathologic study of 120 cases. *Cancer*. 1986; 57: 2006–2021. PMID: 3082508
9. Evans DG, Baser ME, McGaughan J, Sharif S, Howard E, Moran A. Malignant peripheral nerve sheath tumours in neurofibromatosis 1. *J Med Genet*. 2002; 39: 311–314. <https://doi.org/10.1136/jmg.39.5.311> PMID: 12011145
10. Combemale P, Valeyrie-Allanore L, Giammarile F, Pinson S, Guillot B, Goulart DM, et al. Utility of 18F-FDG PET with a semi-quantitative index in the detection of sarcomatous transformation in patients with neurofibromatosis type 1. *PLoS One*. 2014; 9: e85954. <https://doi.org/10.1371/journal.pone.0085954> PMID: 24516522
11. Stucky CC, Johnson KN, Gray RJ, Pockaj BA, Ocal IT, Rose PS, et al. Malignant peripheral nerve sheath tumors (MPNST): the Mayo Clinic experience. *Ann Surg Oncol*. 2012; 19: 878–885. <https://doi.org/10.1245/s10434-011-1978-7> PMID: 21861229
12. Rasmussen SA, Yang Q, Friedman JM. Mortality in neurofibromatosis 1: an analysis using U.S. death certificates. *Am J Hum Genet*. 2001; 68: 1110–1118. <https://doi.org/10.1086/320121> PMID: 11283797
13. Warbey VS, Ferner RE, Dunn JT, Calonje E, O'Doherty MJ. [18F]FDG PET/CT in the diagnosis of malignant peripheral nerve sheath tumours in neurofibromatosis type-1. *Eur J Nucl Med Mol Imaging*. 2009; 36: 751–757. <https://doi.org/10.1007/s00259-008-1038-0> PMID: 19142634
14. Chirindel A, Chaudhry M, Blakeley JO, Wahl R. 18F-FDG PET/CT qualitative and quantitative evaluation in neurofibromatosis type 1 patients for detection of malignant transformation: comparison of early to delayed imaging with and without liver activity normalization. *J Nucl Med*. 2015; 56: 379–385. <https://doi.org/10.2967/jnumed.114.142372> PMID: 25655626
15. Salamon J, Derlin T, Bannas P, Busch JD, Herrmann J, Bockhorn M, et al. Evaluation of intratumoural heterogeneity on ¹⁸F-FDG PET/CT for characterization of peripheral nerve sheath tumours in neurofibromatosis type 1. *Eur J Nucl Med Mol Imaging*. 2013; 40:685–692. <https://doi.org/10.1007/s00259-012-2314-6> PMID: 23232507
16. Derlin T, Tornquist K, Münster S, Apostolova I, Hagel C, Friedrich RE, et al. Comparative effectiveness of 18F-FDG PET/CT versus whole-body MRI for detection of malignant peripheral nerve sheath tumors in neurofibromatosis type 1. *Clin Nucl Med*. 2013; 38: e19–25. <https://doi.org/10.1097/RLU.0b013e318266ce84> PMID: 23242059
17. Benz MR, Czernin J, Dry SM, Tap WD, Allen-Auerbach MS, Elashoff D, et al. Quantitative F18-fluorodeoxyglucose positron emission tomography accurately characterizes peripheral nerve sheath tumors as malignant or benign. *Cancer*. 2010; 116: 451–458. <https://doi.org/10.1002/cncr.24755> PMID: 19924789
18. Adams MC, Turkington TG, Wilson JM, Wong TZ. A systematic review of the factors affecting accuracy of SUV measurements. *AJR Am J Roentgenol*. 2010; 195: 310–320. <https://doi.org/10.2214/AJR.10.4923> PMID: 20651185
19. Azizi AA, Slavc I, Theisen BE, Rausch I, Weber M, Happak W, et al. Monitoring of plexiform neurofibroma in children and adolescents with neurofibromatosis type 1 by [18F]FDG-PET imaging. Is it of value in asymptomatic patients? *Pediatr Blood Cancer*. 2017. doi: 10.1002.
20. Salamon J, Veldhoen S, Apostolova I, et al. 18F-FDG PET/CT for detection of malignant peripheral nerve sheath tumours in neurofibromatosis type 1: tumour-to-liver ratio is superior to an SUVmax cut-off. *Eur Radiol*. 2014; 24: 405–412. <https://doi.org/10.1007/s00330-013-3020-x> PMID: 24097302
21. Van Der Gucht A, Zehou O, Djelbani-Ahmed S, Valeyrie-Allanore L, Ortonne N, Brugières P, et al. Metabolic Tumor Burden Measured by 18F-FDG PET/CT Predicts Malignant Transformation in Patients with Neurofibromatosis Type-1. *PLoS One*. 2016; 11: e0151809. <https://doi.org/10.1371/journal.pone.0151809> PMID: 26987124
22. Chirindel A, Alluri KC, Tahari AK, Chaudhry M, Wahl RL, Lodge MA, et al. Liver standardized uptake value corrected for lean body mass at FDG PET/CT: effect of FDG uptake time. *Clin Nucl Med*. 2015; 40: e17–22. <https://doi.org/10.1097/RLU.0000000000000446> PMID: 24873794

23. Schaarschmidt BM, Buchbender C, Nensa F, Grueneisen J, Gomez B, Kehler J, et al. Correlation of the apparent diffusion coefficient (ADC) with the standardized uptake value (SUV) in lymph node metastases of non-small cell lung cancer (NSCLC) patients using hybrid 18F-FDG PET/MRI. *PLoS One*. 2015; 10: e0122545. <https://doi.org/10.1371/journal.pone.0122545> PMID: 25807190
24. Grueneisen J, Beiderwellen K, Heusch P, Buderath P, Aktas B, Gratz M, et al. Correlation of Standardized Uptake Value and Apparent Diffusion Coefficient in Integrated Whole-Body PET/MRI of Primary and Recurrent Cervical Cancer. *PLoS ONE*. 2014; 9: e96751. <https://doi.org/10.1371/journal.pone.0096751> PMID: 24804676
25. Rakheja R, Chandarana H, DeMello L, Jackson K, Geppert C, Faul D, et al. Correlation Between Standardized Uptake Value and Apparent Diffusion Coefficient of Neoplastic Lesions Evaluated With Whole-Body Simultaneous Hybrid PET/MRI. *Am J Roentgenol*. 2013; 201: 1115–1119.
26. Ohno Y, Koyama H, Yoshikawa T, Matsumoto K, Aoyama N, Onishi Y, et al. Diffusion-Weighted MRI Versus 18F-FDG PET/CT: Performance as Predictors of Tumor Treatment Response and Patient Survival in Patients With Non-Small Cell Lung Cancer Receiving Chemoradiotherapy. *Am J Roentgenol*. 2012; 198: 75–82.
27. Mayerhoefer ME, Karanikas G, Kletter K, Kiesewetter B, Weber M, Rausch I, et al. Can Interim 18F-FDG PET or Diffusion-Weighted MRI Predict End-of-Treatment Outcome in FDG-Avid MALT Lymphoma After Rituximab-Based Therapy?: A Preliminary Study in 15 Patients. *Clin Nucl Med*. 2016; 41: 837–843. <https://doi.org/10.1097/RLU.0000000000001395> PMID: 27648705